Using 1,1,1-Trichloroethane degradation data to understand NAPL dissolution and solute transport at real sites

Valeureux Illy, Gregory J.V. Cohen, Elicia Verardo, Patrick Höhener, Nathalie Guiserix, Olivier Atteia

Using 1,1,1-Trichloroethane degradation data to understand NAPL dissolution and solute transport at real sites

Valeureux D. Illy[a,b,*], Gregory J. V. Cohen[a], Elicia Verardo[a], Patrick Höhener[c], Nathalie Guiserix[b], Olivier Atteia[a]

[a] *EA 4592, Géoressources et Environnement, Bordeaux INP, Université Bordeaux Montaigne, 1 Avenue Dr Schweitzer, 33400 Talence, France*

[b] *Renault SAS, 1 Allée du Golf, Guyancourt 78 280, France*

[c] *Laboratoire de Chimie Environnementale-UMR 7376, Aix-Marseille Université-CNRS, 3 place Victor Hugo - Case 29, 13331 Marseille Cedex 3*

*Author for correspondence: valeureux.illy@gmail.com or valeureux.illy@bordeaux-inp.fr

Tel: +33 6 37 74 19 51
Fax: +33 5 57 12 10 01

Highlights

- Using TCA hydrolysis constant to age date of pollution release to groundwater
- TCA hydrolysis kinetic constant is between $2.7.10^{-4}$ d^{-1} and $3.0.10^{-4}$ d^{-1}
- Understanding NAPL dissolution to predict solute concentrations
- Aquifer is heterogeneous and first spill dates to 1990

Abstract

Analytical and numerical models describing the evolution of contaminant concentrations in the plume associated with the dissolution of NAPL source and degradation processes were presented in the literature. At real sites and particularly in complex aquifers like chalk, it is difficult to understand how the sources of contaminants evolve with time.

1,1,1-Trichlorethane (1,1,1-TCA) is one of the few compounds with a well-known hydrolysis constant, that can help to improve knowledge of the contaminant sources and transport rates of dissolved contaminants in groundwater by dating the spill.

In this work, different scenarios that could explain the evolution of the concentrations of 1,1,1-TCA and its degradation product 1,1-Dichloroethene (1,1-DCE) at a real contaminated site were investigated by analytical and numerical modelling.

The results show that (1) the peaks of concentration time series do not correspond to a single contamination event even in the case of a complex medium, (2) the multiphasic behavior of the concentration time series is dictated by the dissolution in a heterogeneous medium, and (3) the persistence of the concentrations can arise from a small residual organic phase or transport in dual domain medium.

Keywords

NAPL
Dissolution
Hydrolysis
1,1,1-Trichloroethane
Analytical model
Numerical model

1. Introduction

Halogenated Volatile Organic Compounds (HVOCs) such as 1,1,1-TCA (TCA) are Dense Non Aqueous Phase Liquids (DNAPLs) and are among the most frequently encountered pollutants in groundwater at industrial sites (Bost and Perry 2006; Plumb Jr 1992). This situation is explained by their uses in various industrial activities, in particular dry cleaning and degreasing of metal parts (Kota et al. 2003; Scheutz et al. 2011a). TCA in particular has been used extensively for more than 35 years (between 1960 and 2000) as a replacement for TCE and PCE because of their danger to the environment and human health (Lawrence 2006; Morrison and Murphy 2002; Snyder 1990). These compounds and their degradation products are still found in the environment, especially near older industrial sites where chlorinated solvents were used. These sites are often subject to monitoring of concentrations in the vadose zone and in groundwater, and in certain cases of pollution treatment (Löffler and Edwards 2006; Major et al. 2002; McCarty 1997; Scheutz et al. 2008).

As part of monitoring and remediation programs, adopting an adequate strategy requires a good understanding of (1) the functioning of the contamination source itself and (2) the parameters that determine the persistence of these contaminations several decades after the use of these products has ceased.

In groundwater, the degradation of TCA can occur biotically or abiotically (Broholm et al. 2014; Grostern and Edwards 2006; Palau et al. 2014, 2016; Scheutz et al. 2011a). Biological degradation occurs either by aerobic bacteria by catabolism (Hashimoto et al. 2002), either by anaerobic bacteria (methanogens for example) and sulphate reducing bacteria leading to TCA transformation into 1,1-DCA and then often into Chloroethane (Adamson and Parkin 1999; Bae and Lee 2010; Cho and Choi 2010; De Best et al. 1999; Fennelly and Roberts 1998; Gander et al. 2002; Grostern and Edwards 2006; Sun et al. 2002, 2002). Under these conditions, the degradation kinetics can be limited by the presence of co-contaminants such as PCE and TCE (Duhamel et al. 2002; Grostern and Edwards 2009, 2006). Abiotically, TCA can be degraded by hydrolysis with production of acetate, HCl and 1,1-DCE (Scheutz et al. 2011). The kinetic rates of hydrolysis are higher than reductive dechlorination processes by about a factor of 5, with a yield varying between 73 and 80 % for the production of acetate and 20 to 27 % for 1,1-DCE (Cline and Delfino 1989; Ellenrieder and Reinhard 1988; Gerkens and Franklin 1989; Haag and Mill 1988; Vogel and McCarty 1987; Wing 1997). These different degradation pathways were demonstrated and differentiated by isotopic approaches on $\delta^{13}C$ and $\delta^{37}Cl$ (Abe et al. 2009; Elsner et al. 2008; Hunkeler et al. 2008; Palau et al. 2016, 2014; VanStone et al. 2008).

In groundwater, the concentrations of TCA and 1,1-DCE dissolved in the plume depend on the hydrolysis kinetics which are generally pseudo first order if the pH of the medium is lower than 11 (Cline and Delfino 1989; Vogel and McCarty 1987; Wing 1997). The yield is generally independent of the temperature and the pH of the groundwater under natural environmental conditions (Ellenrieder and Reinhard 1988; Gerkens and Franklin 1989; Haag and Mill 1988). This offers the interesting possibility to use the ratio of 1,1-DCE to TCA as a clock to estimate the date of the original first pollution by pure TCA (Gauthier and Murphy 2003; Wing 1997).

In the presence of a source zone of DNAPLs, the dissolution kinetics of the organic phase, which determines the concentrations of solutes, depend on several parameters such as the organic phase mass and solubility, groundwater flow rates and dispersivities (Clement et al. 2004; Nambi and Powers 2000; Powers et al. 1992). In a heterogeneous environment, other mechanisms such as the variability of local relative permeability or the DNAPL-water interface area of the source zone also affect the concentrations of solutes in the plume (Christ et al. 2006; DiFilippo et al. 2010; Fure et al. 2006; Lemke and Abriola 2006; Rivett and Allen-King 2003). In contrast, the depletion of the sources of Light Non Aqueous Phase Liquids (LNAPLs) in the vadose zone is also subject to other processes such as volatilization, capillary effects, and water table fluctuation (Davis et al. 2005; Yang et al. 2013; Lari et al. 2019).

The present article focuses on a site contaminated by DNAPLs in the north of France which is regularly monitored for pollutant concentrations in groundwater at the site as well as hydraulic downstream. This monitoring enabled the acquisition of almost 20 years long time series (2002-2020) of TCA and 1,1-DCE concentrations measured immediately downstream of the site. On these concentration time series, several peaks of different shapes and resolutions are observed as well as low concentrations that persist until the present day. In order to determine the NAPL dissolution kinetics and characterize the hydrodynamic of the contaminated aquifer at the site, different analytical and numerical models considering the different processes were applied and the results compared to concentration time series. These models were developed to understand the origin of solutes and the persistence of these contaminants in groundwater two decades after their use ceases. This may allow predicting future changes in concentrations.

The major objective of the paper is to use the degradation properties of TCA to determine whether the different peaks observed are the result of distinct contamination events or

different migration pathways, if TCA was present as a NAPL or dissolved source at the entry point of the water table, and if it is possible to precisely date the origin of the contamination.

2. Materials and methods

2.1. Study area and hydrogeology

The study site is a factory producing motor vehicles since 1970. It houses buildings dedicated to stamping, painting, storage, and logistics activities. The site is located on Quaternary silts lying on the Senonian chalks aquifer with a thickness of about 65 m. In the well cores, the presence of fractures was identified. The impermeable substratum includes marls of the Middle and Lower Turonian (Figure 1).

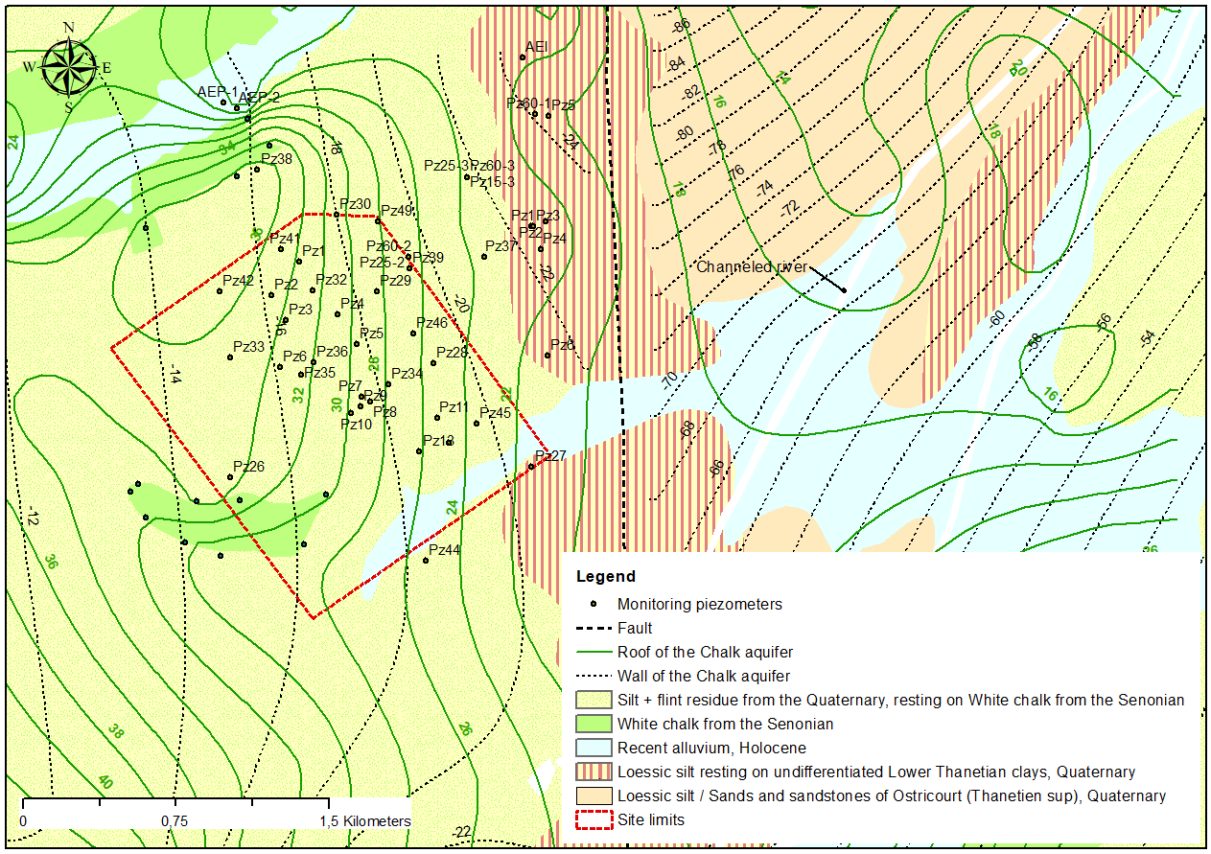

Figure 1 : Map of the geology of the study site showing the level of the roof and chalk wall and the surface formations that cover the chalk (Lexman 2016)

At the site, the groundwater globally flows from the southwest to the northeast with an average hydraulic gradient of 1.5 ‰ (Figure 2). A total porosity between 0.25 and 0.38 was measured with a mercury porosimeter on cores from boreholes drilled in 2020.

Soil surveys carried out between 0 and 5 m deep, between 2002 and 2018, enabled the source zones delineation. The two most important sources of TCA are located next to the paint

dilution building and the south end of sheet metal building. These two source zones were well known for the risk of contamination. Indeed, the source zone of the CA building is a paint dilution area, and the source zone of the "Sheet metal" building is the location of a former metal parts degreasing station where 1,1,1-TCA was used (trade name ATOCHEM). The investigations confirmed an impact of 1,1,1-TCA in the soil under (Figure S 1 of the Supporting Information).

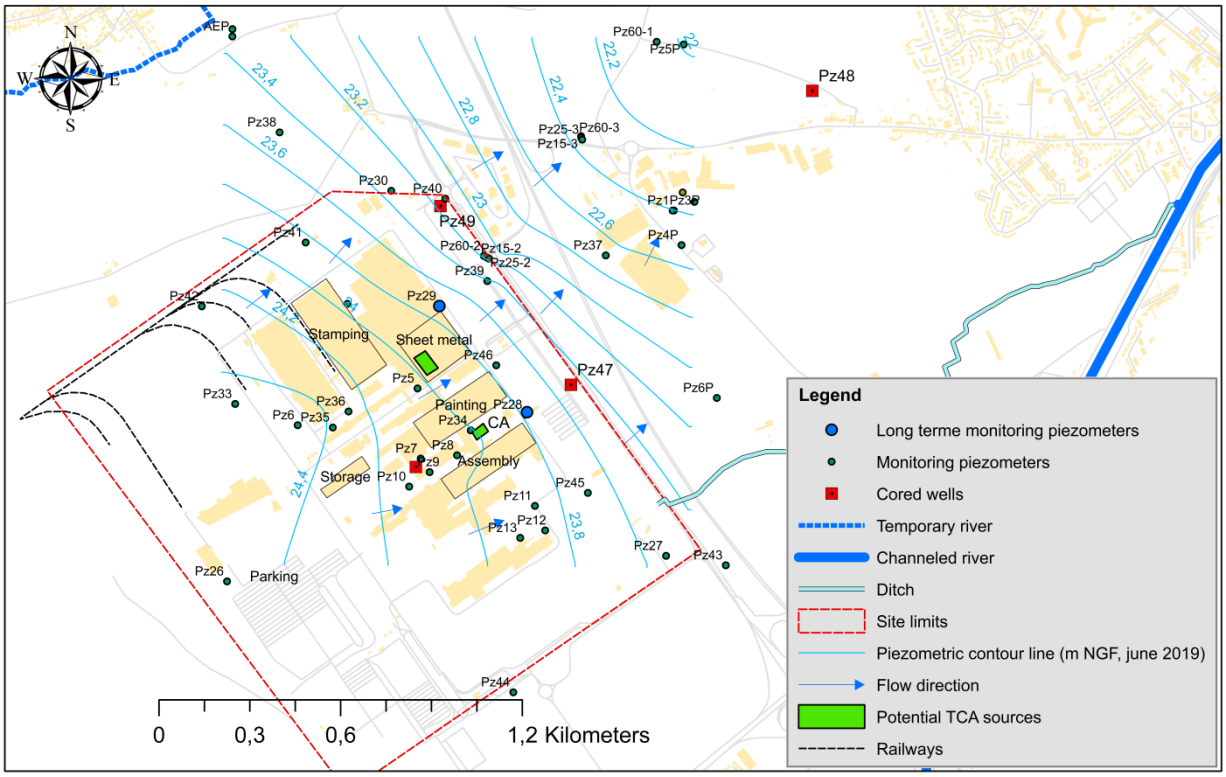

Figure 2 : Site map and location of the piezometers. The green rectangles indicate the location of identified sources of TCA. The red squares indicate the cored wells. The blue circles show the monitored piezometers location. The blue arrow indicates the general flow direction.

Analysis of the physicochemical parameters shows for all the piezometers (except for Pz9) a dissolved oxygen level between 1 and 10 mg/L and a redox potential that varies between 100 and 220 mV. The detailed physicochemical parameters and the concentrations of the major ions are provided in Table S 1 of the Supporting Information.

2.2. **Contamination and concentration time series**

A contamination of groundwater by chlorinated solvents has been detected at the site in 2002 and concentration monitoring has been set up since. The plant has stopped using TCA and

similar products since 2000. However, 20 years after this product replacement, TCA and its degradation product, 1,1-DCE, are still quantified in the underlying aquifer.

Groundwater was sampled during the years by several companies and in accordance with French standard FD X 31-615 of December 2000 relating to sampling of groundwater in a borehole. The piezometers were always purged, and the physicochemical parameters monitored until stabilization before sampling. The samples were then placed in clean bottles provided by the laboratory, stored and transported at 3-4 °C protected from light until they arrived in the cold room of the laboratory. The analyses were carried out by several laboratories with French COFRAC accreditation.

The quantification limits for TCA and 1,1-DCE have remained constant since 2002 and are 0.5 µg/L (*i.e.*, $3.5.10^{-9}$ and $5.16.10^{-9}$ mol/L for TCA and 1,1-DCE, respectively).

The concentration time series at Pz28 and Pz29, close to sources of contamination are presented in Figure 3.

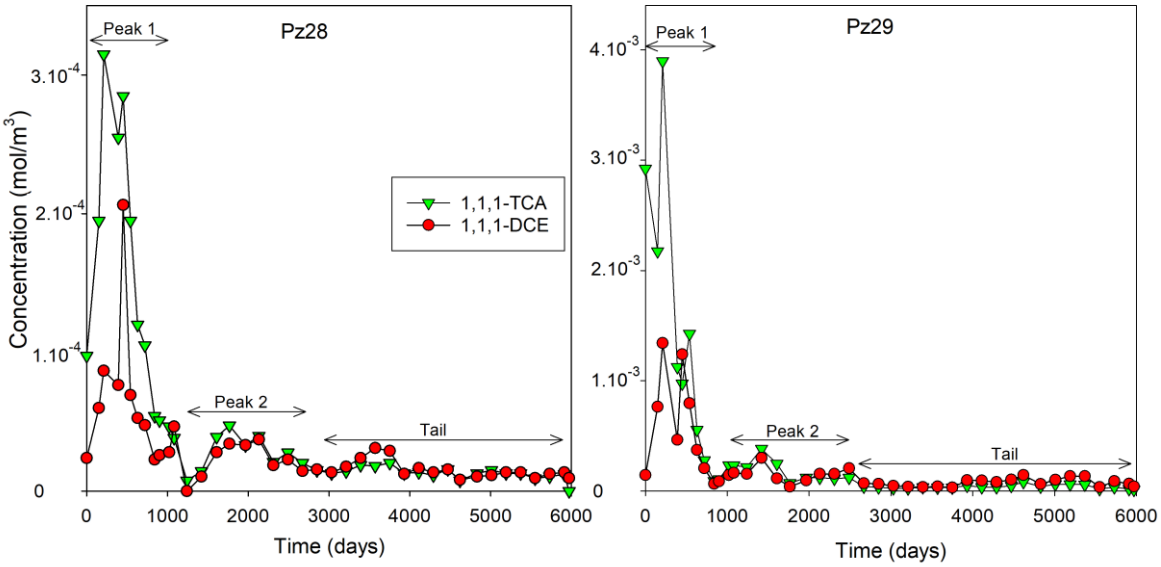

Figure 3 : Temporal evolution of TCA and 1,1-DCE concentrations at Pz28 and Pz29 wells since 2002, highlighting the peaks and the tail of low concentrations.

On these figures, 2 peaks of different shapes can be observed. Between 0 and 1000 days, a first thin peak of high amplitude (maximum measured concentrations of 3.10^{-7} and 4.10^{-6} mol/L on Pz28 and Pz29, respectively) was observed. Following this first peak a second smaller peak (maximum measured concentrations of 6.10^{-8} and 5.10^{-7} mol/L on Pz28 and Pz29, respectively) occurred in the interval between 1000 and 2500 days. Then, the measured concentrations evolved between 1.10^{-8} and 8.10^{-8} mol/L in Pz29 and between 7.10^{-9} and 2.10^{-8} mol/L in Pz28. These low concentrations (a few µg/L) persist until now.

2.3. **Estimated errors on concentrations and ratio 1,1-DCE to TCA**

The quantification limits induce errors on the calculated 1,1-DCE/TCA ratios. These errors are higher as the measured concentrations are close to these limits. The uncertainties ΔR on the 1,1-DCE/TCA ratios were therefore calculated using errors propagation method.

$$\Delta R = \frac{C_w^{DCE}}{C_w^{TCA}} \sqrt{\left(\frac{\Delta_{DCE}}{C_w^{DCE}}\right)^2 + \left(\frac{\Delta_{TCA}}{C_w^{TCA}}\right)^2}, \quad (1)$$

where:

- Δ_{DCE} and Δ_{TCA} are the absolute uncertainties, considered equal to the limits of quantification of 1,1-DCE and TCA respectively.
- C_w^{DCE} and C_w^{TCA} are the measured concentrations of DCE and TCA respectively.

As shown by Wing (1997), and since transformation of TCA on the studied site is mainly dehydrohalogenation and hydrolysis, the rate of transformation can be expressed as :

$$\ln\left(1 + 4\frac{C_w^{DCE}(t)}{C_w^{TCA}(t)}\right) = k_{deg}t \quad (2)$$

The constant 4 comes from the 25% yield of 1,1-DCE produced by TCA transformation (Ellenrieder and Reinhard 1988; Gerkens and Franklin 1989; Haag and Mill 1988; Vogel and McCarty 1987; Wing 1997).

2.4. **Modelling assumptions**

Six 2D models were built to reproduce the site configuration as closely as possible, while honoring literature and experimental data. These models were tested in order to find the one that best fits the existing data but also, by comparison, to help understanding the role of each process on the TCA and 1,1-DCE concentrations.

The models present one or two sources which are dissolved or in organic phase and placed in a field of hydraulic conductivity which can be homogeneous (Falta et al. 2005a, 2005b) or heterogeneous (Nambi and Powers 2000; Rivett et al. 2001). The medium can have a unique porosity or a dual domain (Zheng and Wang 1999).

The characteristics of the different models are summarized in Figure 4.

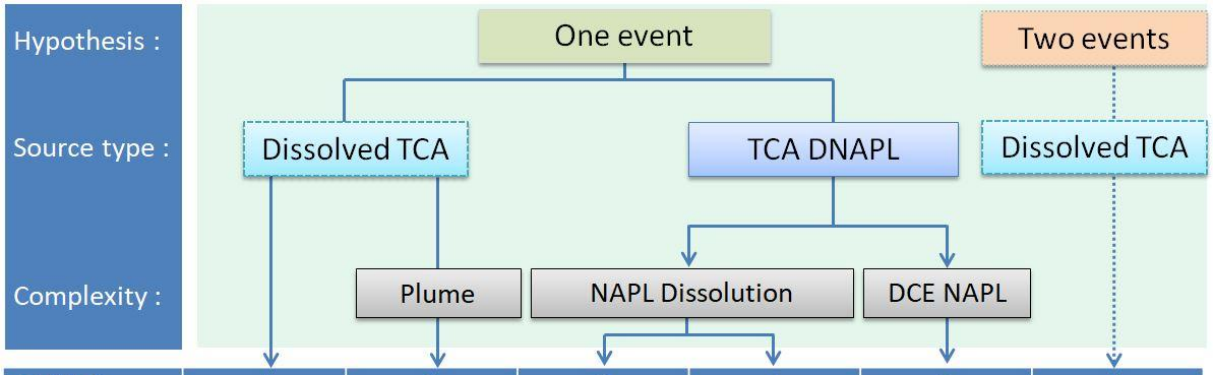

Model n°	1	2	3	4	5	6
Model name	Dissolved TCA in a homogeneous aquifer	Dissolved TCA in a « dual domain » aquifer	TCA NAPL in a homogeneous source zone	TCA NAPL in a heterogeneous source zone	TCA + DCE NAPL in a heterogeneous source	Dissolved TCA in two contamination events
Model type	**analytic**	numeric	numeric	numeric	numeric	**analytic**
Hydraulic conductivity field (K)	homogeneous	homogeneous	homogeneous	**heterogeneous**	**heterogeneous**	homogeneous
Porosity field (θ)	homogeneous	**double porosity**	homogeneous	homogeneous	homogeneous	homogeneous

Figure 4 : Characteristics of studied models with the assumptions on the number of contamination event and the type of source.

2.4.1. NAPL dissolution

Dissolution of NAPLs occurs at the interface of water and NAPL. It is assumed here, as in literature (Lemke and Abriola 2006; Powers et al. 1994; Zhu and Sykes 2004), that the linear driving force expression is appropriate to represent the inter-phase mass transfer flux (J^0) :

$$J^0 = \lambda(C_{WSAT} - C_W), \quad (3)$$

where λ is the mass transfer coefficient, C_{WSAT} is the aqueous equilibrium concentration (solubility) and C_W is the concentration (of TCA) in the aqueous phase.

Dissolution from a heterogeneous source was also considered. The heterogeneous source consists in an area with a part located in a low permeability (lowK) zone and the rest having the same permeability as the whole domain (globK).

Model 3 to 5 include a NAPL source. In model 5, 1,1-DCE is considered to partition back in the NAPL once it has been produced by TCA degradation, like shown for instance by Ramsburg et al. (2010) for other substances. As the proportion of DCE is difficult to know, it was assumed to be at equilibrium with the dissolved phase, considering aqueous dissolution following Raoult's law.

2.4.2. Transport and degradation of solutes

2.4.2.1. Analytical models (model 1 and 6)

In the simplest approach, the transport is considered to occur in a homogeneous medium which leads to a 2D analytical equation for the injection of a mass at time 0 with a pore velocity *v* in the *x* direction, given by equation (4) (Bear 2012):

$$C(x,y,t) = \frac{M_0/\theta}{4\pi vt\sqrt{\alpha_L \alpha_T}} exp\left(-\frac{(x-vt)^2}{4\alpha_L vt} - \frac{y^2}{4\alpha_T vt}\right) \exp\left(-k_{deg}t\right) \quad (4)$$

with:

- M_0: the injected mass.
- θ: the effective porosity of the medium.
- α_L and α_T: the longitudinal and transverse dispersivities.
- k_{deg} is the degradation constant of TCA.

The concentration of TCA and 1,1-DCE can be calculated iteratively in a spreadsheet, using first-order kinetics (Battersby 1990; Wing 1997):

$$\frac{dC_w^{TCA}}{dt} = -k_{deg}C_w^{TCA}, \quad (5)$$

which implies:

$$C_w^{TCA}(t) = C_w^{TCA}(0)\exp\left(-k_{deg}.t\right) \quad (6)$$

$$C_w^{DCE}(t) = C_w^{TCA}(0)[1-\exp\left(-k_{deg}.t\right)]r_H \quad (7)$$

where:

- r_H is the yield of 1,1-DCE coming from the TCA aerobic degradation,
- $C_w^{TCA}(t)$, $C_w^{DCE}(t)$ are the dissolved TCA and 1,1-DCE concentration at time t.

2.4.2.2. Numerical models (model 2, 3, 4 and 5)

The equations were solved with the MT3DMS code (Zheng and Wang 1999) using TVD for the advective scheme. The grid, the boundary conditions and the flow field are presented in the Supporting Information. Degradation of TCA is considered by specifying a first order rate. Dual domain mass transfer has been used in numerous publications to represent the mass exchange between matrices and fissures (Briggs et al. 2014; Falta 2003; Greskowiak et al. 2010; Neumann et al. 2008; Zheng and Wang 1999).

The model consists of two domains: the immobile or matrix domain porosity (θ_{im}) and the mobile or fracture domain porosity (θ_m). The exchanges between the two compartments occur through an exchange coefficient (ζ). Leading to the following formulation (Zheng and Wang 1999):

$$\theta_m \frac{\partial C_m}{\partial t} + \theta_{im} \frac{\partial C_{im}}{\partial t} = \frac{\partial}{\partial x_i}\left(\theta_m D_{ij} \frac{\partial C_m}{\partial x_j}\right) - \frac{\partial C_m}{\partial t}(\theta_m v_i C_m) + q_s C_s - q_s' C_m - k_{deg}\theta_m C_m - k_{deg}\theta_{im} C_{im} \quad (8)$$

The mass conservation implies:

$$\theta_{im} \frac{\partial C_{im}}{\partial t} = \zeta(C_m - C_{im}) - k_{deg}\theta_{im} C_{im} \quad (9)$$

where:

C_m and C_{im} are respectively the concentration in the mobile and immobile domain,

θ_m and θ_{im} are respectively the mobile and immobile porosities,

k_{deg} is the degradation rate present in both domains,

ζ is the rate of transfer between the domains.

Although largely used, this method may have some limitations (Karadimitriou et al. 2016).

The Figure 5 is a conceptual representation of the set of models.

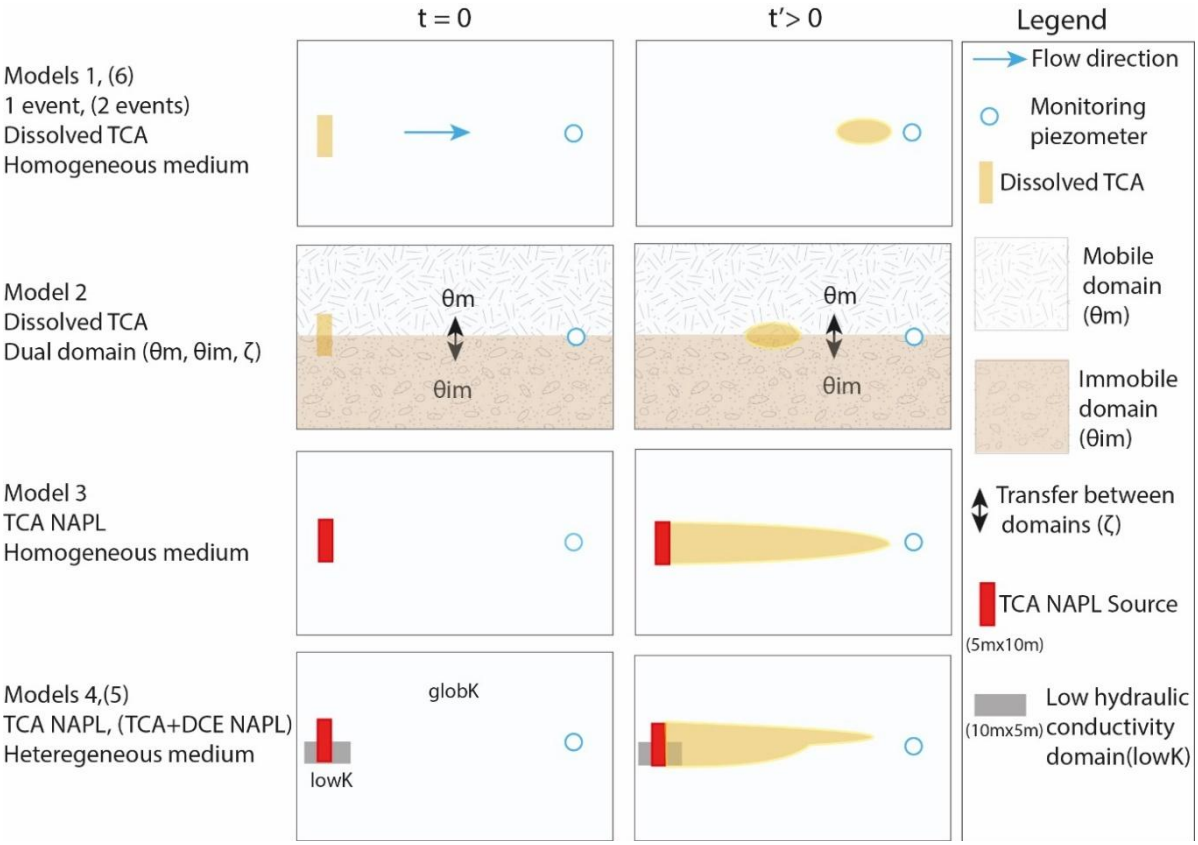

Figure 5 : Conceptual representation of the models. On the left (t=0), the conceptual models at the beginning of the contamination, and on the right (t>0) the conceptual models later in time with transport.

2.4.3. Model parameters

For all models, the yield of 1,1-DCE (r_H) is 0.25, as discussed previously in section (2.3). The distance between the source and the piezometer was set at 150 m as indicated by the results of the delimitation of the source zones on the site. For the transport models, the hydraulic gradient of the domain was set at 1.5 ‰ in accordance with the piezometric maps at the site. The dispersivity values used in all models were obtained by optimization on the basis of the assumptions of model 1. The longitudinal and transverse dispersivities obtained are 30 m and 3 m respectively. These quite large values of dispersivities may come from the fact that the TCA peak last quite long from a supposed unique spill event. It is possible that several events occurred during a short period and mixing of these events will result in one broader peak. The other reason come from the presence of well screened over 15 to 60 m which lead to vertical mixing and thus a higher apparent dispersivity.

Table 1 summarizes the rest of the parameters of each model.

295 **Table 1 : Summary of optimized model parameters; the parameters in parentheses are for Pz29 when different from Pz28, and in**
296 **square brackets for the second contamination event**

Model number	-	**1**	**2**	**3**	**4**	**5**	**6**
Source type	-	Dissolved TCA	TCA NAPL	TCA NAPL	TCA NAPL	TCA NAPL, DCE NAPL	Dissolved TCA
Source zone hydraulic conductivity	-	homogeneous	homogeneous	homogeneous	heterogeneous	heterogeneous	homogeneous
Characteristics of the plume zone	-	homogeneous	dual domain	homogeneous	homogeneous	homogeneous	homogeneous
Date of spill, from the start of monitoring	(d)	-3700 (-4000)	-3700 (-4000)	-3700 (-4000)	-3700 (-4000)	-3700 (-4000)	-3700 (-4000)
NAPL dissolution rate, λ	(d^{-1})	N.A	N.A	0.003	0.001 (0,05)	0.002 (0.004)	N.A
TCA NAPL mass at t=0	(moles/m^2)	N.A	N.A	0.50	0.50	0.5 (0.9)	N.A
Dissolved TCA mass at t=0	(moles/m^2)	0.03 (0.46)	0.12 (1.00)	0.00	0.15 (1.80)	0.16 (1.70)	[0.21] [(2.70)]
DCE NAPL mass at t=0	(moles/m^2)	N.A	N.A	N.A	N.A	0.3 (0.6)	N.A
Dissolved DCE mass at t =0	(moles/m^2)	0.00	0.03 (0.30)	0.00	0.03 (0.60)	0.04 (0.60)	[0.00]
Global hydraulic conductivity, globK	(m/d)	25.0 (50.0)	15.0 (50.7)	15.0	5.0 (10.0)	5.0 (10.0)	25.0 (50.0)
Low hydraulic conductivity zone, lowK	(m/d)	N.A	N.A	N.A	0.05	0.05	N.A
Immobile porosity, θ_{im}	(-)	N.A	0.20	N.A	N.A	N.A	N.A
Mobile porosity, θ_m	(-)	0.15	0.10 (0.15)	0.15	0.15	0.15	0.15
Rate of transfer, ζ	(d^{-1})	N.A	$2.00.10^{-4}$	N.A	N.A	N.A	N.A

3. Results

3.1. **TCA transformation constant and origin of the contamination dating**

In this paper, following Wing (1997), we consider that 1,1-DCE is not degraded in oxidative conditions, as often considered. Some authors (Ferrey et al. 2004; Scheutz et al. 2011; Wu et al. 2014) showed that 1,1 DCE can be degraded abiotically in presence of iron minerals such as magnetite, iron sulfides, green rusts and pyrite. These iron minerals occur naturally in sediments and are usually quantified by X-ray diffraction studies (Berner 2015; Ferrey et al. 2004; Génin et al. 1998). However, and even though we did not perform a mineralogical study on the chalk matrix, data of total trace element concentrations including iron in the groundwater of the studied area (Table S2, Supporting Information) suggest that concentrations of iron minerals in the chalk matrix are very low.

Figure 6 shows the observed temporal evolution of the ratio represented for the two piezometers Pz28 and Pz29, both located downstream of the site. The ratios in the graphs were increasing approximately linearly from 0.5 to 2 and 2.5, for Pz28 and Pz29, respectively. Beyond that (between 4000 and 6000 days), the increase in the ratio became smaller for Pz29 and stabilized for Pz28.

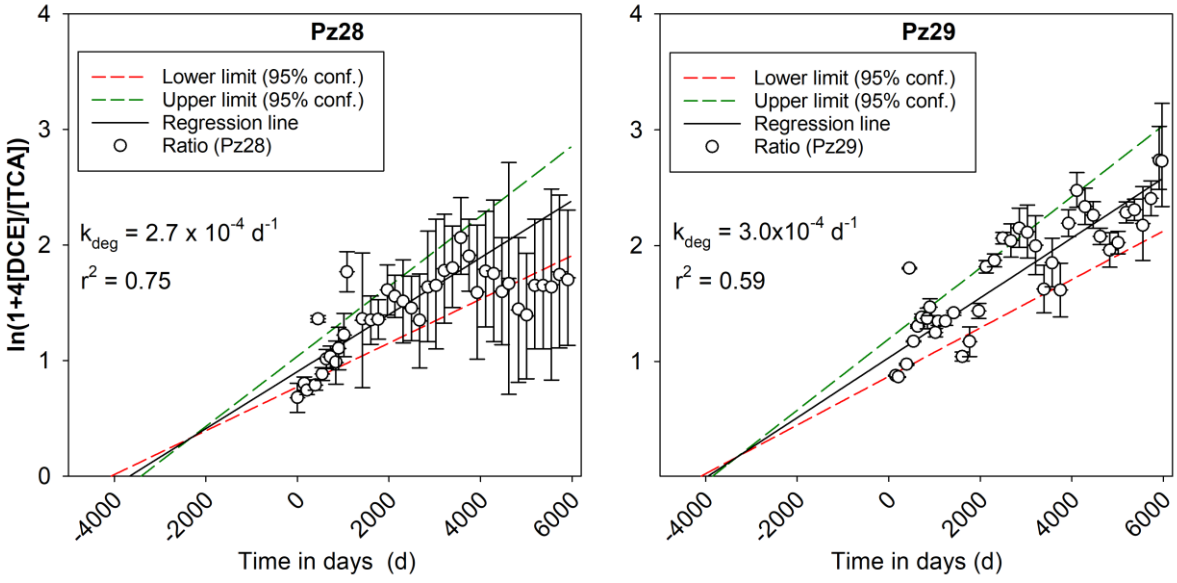

Figure 6 : Estimation of 1,1,1-TCA transformation constant and origin of the contamination

The fitted slope is slightly higher at Pz29 than Pz28. However, the uncertainties in the fitting suggest that these values are not statistically different. It can also be seen that at Pz28 the

slope is higher in the period 0-1500 days, then almost flat from 4000 to 6000 days. For Pz29 there are quite important variations of the slope with no evident reasons for these variations.

As 1,1-DCE is formed from the hydrolysis of TCA, the 1,1-DCE/TCA ratio can be used to determine the age of TCA release (Gauthier and Murphy 2003; Wing 1997).

Wing (1997) has shown that the intersection point of the ratio regression line with the time axis gives a good estimate of the origin of the contamination. The Figure 6 shows that these intersection points are roughly the same on Pz28 and Pz29, which consolidates the contamination dating estimate. It is about -4000 days from the start of monitoring, corresponding to approximately 11 years before the start of monitoring which dates to 1991.

It is important in making this estimate to take into account the uncertainties of the concentrations on the calculated ratios (Gauthier and Murphy 2003). The uncertainty of the estimate is equal to 8 months and 1.8 years based on data from Pz28 and Pz29 respectively. This origin which predates the start of the concentration measurements on the piezometers (time 0, Figure 5) explains the fact that the 1,1-DCE/TCA ratios were already high at the beginning of the measurements (approximately 0.7).

3.2. **Model results**

3.2.1. Model 1: Source is pure dissolved TCA

The transport parameters of the equation (3) were optimized through the Excel solver, which leads to a good fit of the main peak of TCA and 1,1-DCE at both wells. As a result, the Root Mean Square Error (RMSE)of the ratios is less than 0.5.

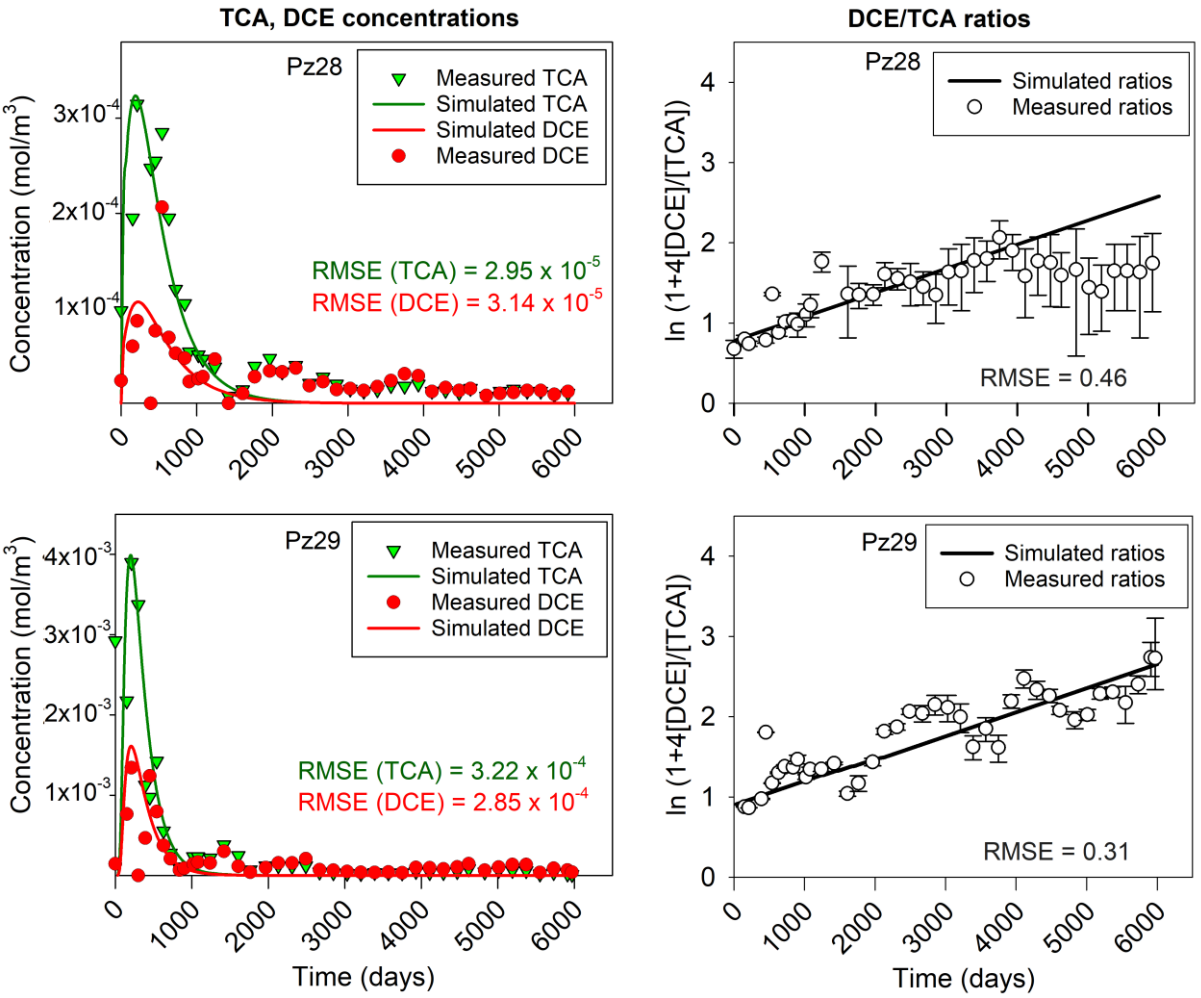

Figure 7 : Concentrations of TCA, DCE and DCE / TCA ratios measured on Pz28 and Pz29 compared to the values simulated with model 1 under the hypothesis of TCA fully dissolved in a homogeneous medium.

The ratio is also quite well fitted, the major issue arises from long term concentrations that are null in the model while the measured ones are around 10^{-8} mol/L, *i.e.*, around the regulatory values.

3.2.2. Model 2: "Dual domain" model: Source is pure dissolved TCA in a double porosity medium.

In the case of a dual domain medium, the TCA of the mobile zones is quickly mobilized leading to a concentration peak which starts to decrease after the exhaustion of TCA in the mobile zone. However, the TCA of the immobile zone is exchanged by diffusion with the mobile zone (Wefer-Roehl et al. 2001) and has the effect of an extension of the tail of the concentration peak (Figure 8) unlike the case of homogeneous media in which the concentrations decrease rapidly after the peak.

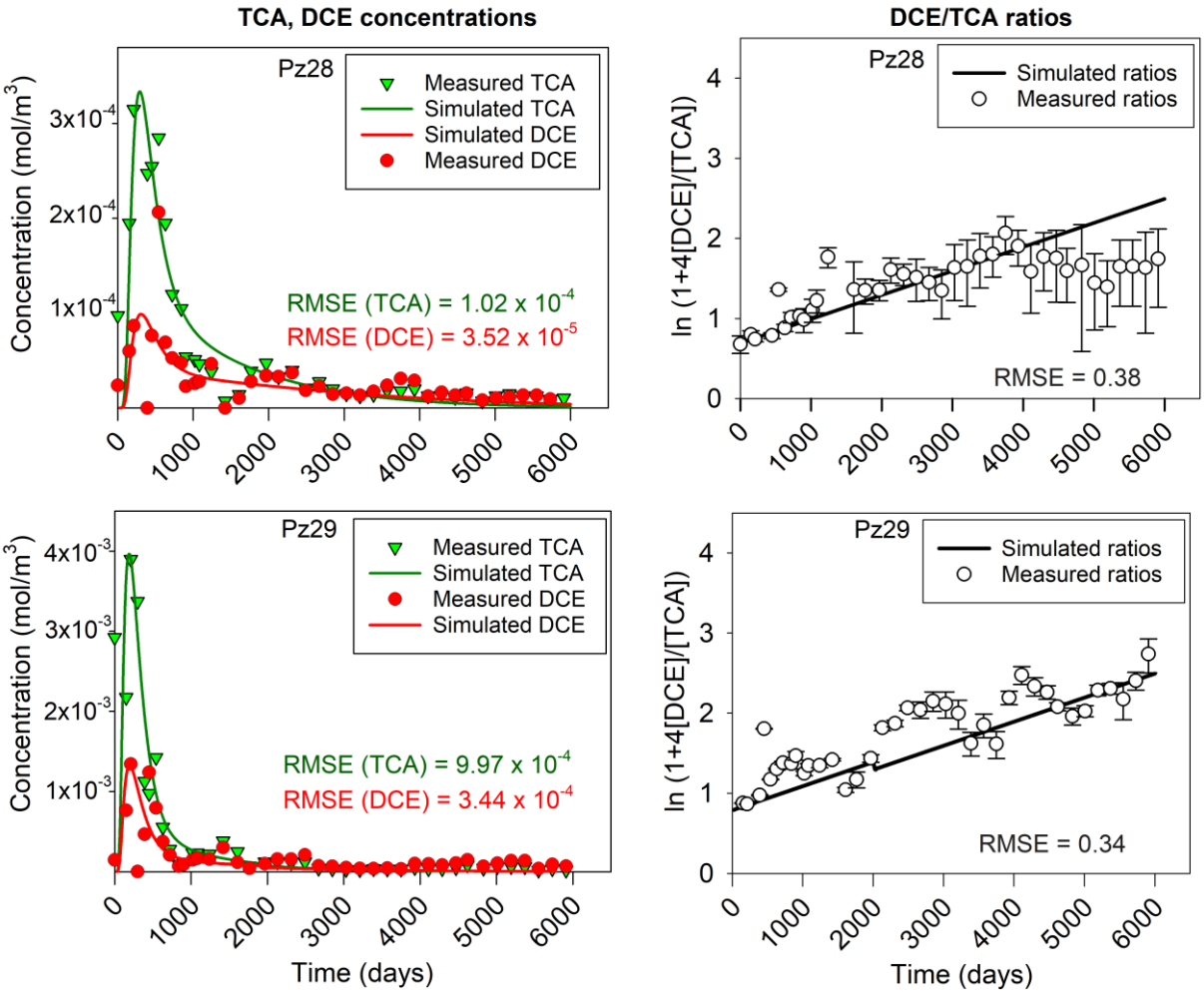

Figure 8 : Measured concentrations of TCA, DCE and DCE / TCA ratios compared to the values simulated by model 2 under the assumption of a dual domain.

3.2.3. Model 3: NAPL source, homogeneous domain

In a homogeneous medium, a NAPL source gives concentrations in the plume which reach equilibrium (Figure 9). Consequently, the 1,1-DCE/TCA ratio is constant after the equilibrium point. With a simple organic source both the concentrations and ratio are not correctly fitted. The model 3 is therefore disqualified and not further discussed.

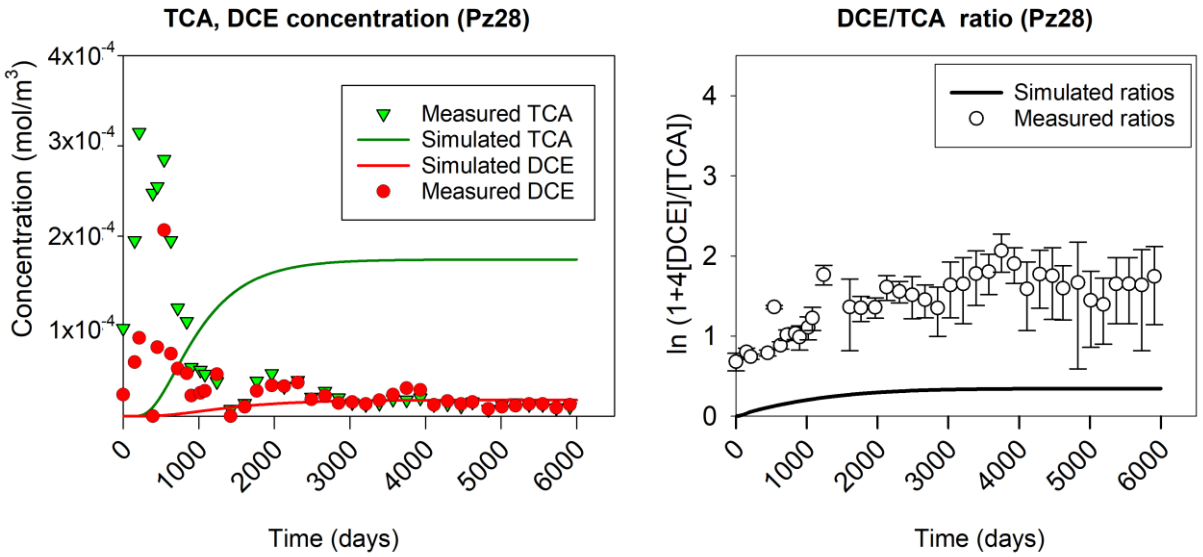

Figure 9 : Measured concentrations of TCA, DCE and DCE / TCA ratios compared to the values simulated by model 3 with the assumption of a DNAPL source in a homogeneous medium.

3.2.4. Models 4 (TCA NAPL only) and 5 (TCA NAPL and 1,1-DCE NAPL) in a heterogeneous hydraulic conductivity medium with single porosity.

In a heterogeneous medium with TCA NAPL source (model 4), it is observed that the concentrations of the dissolved species in the plume resulting from the dissolution of a source of NAPL vary with time and consequently the 1,1-DCE/TCA ratio experiences periods of growth, decrease and stabilization (continuous curves in Figure 10).

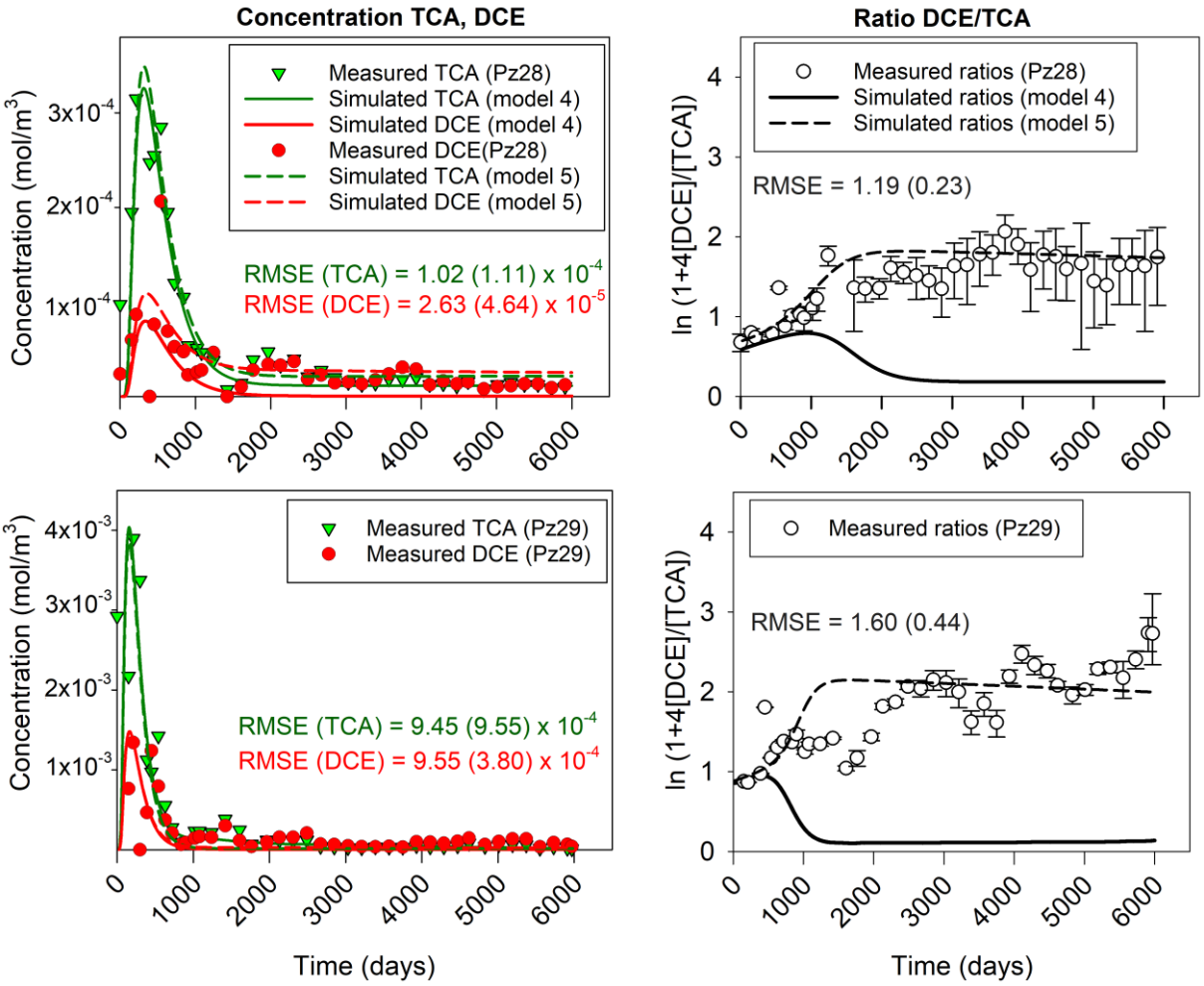

Figure 10 : Measured concentrations of TCA, DCE and DCE/TCA ratios compared to the simulated values (the continuous curves correspond to model 4 and the dashed curves to model 5). RMSE for model 5 are in brackets.

The calibrated dissolution constant leads to a very fast dissolution of the part of the source located in the globK part and thus a peak equivalent to a dissolved source. Then, the dissolution is much slower as the flow passing through the lowK zone is very low, leading to low concentrations that last until NAPL remains.

With the presence of a source of 1,1-DCE (model 5), the 1,1-DCE / TCA ratio remains higher for a long time.

3.2.5. Model 6: Source of dissolved TCA in two events

Previous models show that with a single contamination event, the second peak in concentrations is not reproducible. In the hypothesis of a double contamination separated in time, with the first peak at 210 days and the second peak at 1760 days and 1320 days for Pz28 and Pz29 respectively, one obtains a reproduction of the two peaks (Figure 11).

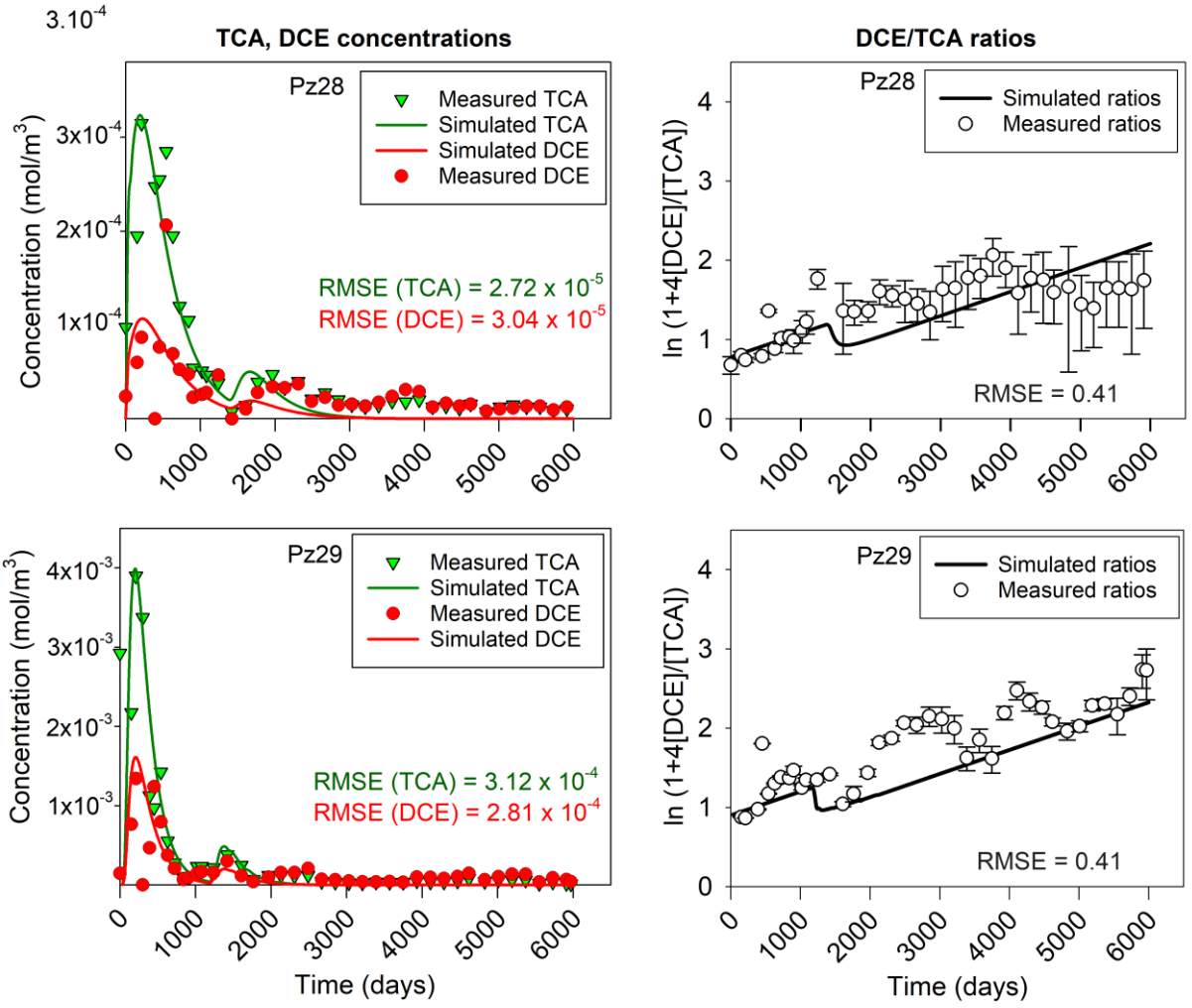

Figure 11 : Measured concentrations of TCA, DCE and DCE / TCA ratios compared to values simulated with model 6 under the assumption of a two events contamination.

Under these conditions, the ratio increases with time and there is a sharp drop followed by a resumption of linear growth.

The RMSE of the different models in relation to the observed data is presented in the Table 2.

402 **Table 2 : Summary of RMSE TCA, 1,1-DCE and the 1,1-DCE/TCA ratio for the different models**

Model number	1	2	3	4	5	6
Model name	Dissolved TCA in homogeneous source	Dissolved TCA in dual domain	TCA NAPL in homogeneous source	TCA NAPL in heterogeneous source	1,1-DCE + TCA NAPL in heterogeneous source	Dissolved TCA in 2 events contaminations
TCA, Pz28	2.95×10^{-5}	1.02×10^{-4}	N. A	1.02×10^{-4}	1.11×10^{-4}	2.72×10^{-5}
TCA, Pz29	3.22×10^{-4}	9.97×10^{-4}	N. A	9.45×10^{-4}	9.55×10^{-4}	3.12×10^{-4}
1,1-DCE, Pz28	3.14×10^{-5}	3.52×10^{-5}	N. A	2.63×10^{-4}	4.64×10^{-5}	3.04×10^{-5}
1,1-DCE, Pz29	2.85×10^{-4}	3.44×10^{-4}	N. A	9.55×10^{-4}	3.80×10^{-4}	2.81×10^{-4}
Ratio, Pz28	0.46	0.38	N. A	1.19	0.23	0.41
Ratio, Pz29	0.31	0.34	N. A	1.60	0.44	0.41

4. Discussion

4.1. **Comparison of Models**

Model 1 (TCA dissolved in homogeneous medium in a single event, Figure 7) and model 6 (TCA dissolved in homogeneous medium in two events, Figure 11) results show good optimizations on the 1,1-DCE/TCA ratio (RMSE <0.50).

The two-event model 6 also simulates the second peak of concentrations and therefore shows a sharp drop in the ratio at the start of the second event, due to the arrival of a fraction of dissolved TCA not yet degraded. However, for these pure transport models, the low remaining concentrations at the tail after 2000 days are not reproduced.

In contrast with model 1, the dual domain model 2 gives a peak which decreases more slowly. Low concentrations therefore last a little longer than in a homogeneous medium.

The main weakness of models 4 and 5 with dissolved TCA is their inability to account for the low concentrations that persist after peaks. In this, the models in a heterogeneous medium in addition to the first peak being well fitted, give a better fitting of the tail of low concentrations of TCA and DCE.

Models 4 and 5 give very similar changes in concentrations between 0 and 1000 days. However, the post-first peak evolution is more sensitive to the presence or absence of an organic phase of 1,1-DCE in the source. In the case of the presence of an organic phase of 1,1-DCE in the source (model 5), the simulated ratios are closer to the observed values. This suggests the presence in the source zone of an organic phase of 1,1-DCE. This situation could be explained by the return of dissolved 1,1-DCE in the organic phase, which is generated by the affinity of the 1,1-DCE for the organic phase (Ramsburg et al. 2010), or possibly by a degradation of the TCA in the unsaturated zone before the arrival of the contamination in the water table, due to the fact that transfer time through the ZNS is slow (between 0.3 and 0.7 m/year) (Chen et al. 2019).

4.2. **, Evolution of the organic phase and possible explanation of the tail of low concentrations**

Experiments were carried out on the efficiency of the elimination of a source of NAPL in heterogeneous porosity zone and the impact of the non-uniform distribution of the NAPL source zones on the reduction of mass fluxes (Akyol 2018; Akyol et al. 2013; Akyol and Turkkan 2018). The results showed an evolution of mass fluxes in multiple steps. The cause

of this multi-step behavior has been attributed to the heterogeneity of the NAPL source zone. In the initial stage, the organic phase within the matrix is hydraulically accessible and gives rise to high concentrations of solutes as observed at the start of the concentrations time series of Pz28 and Pz29. Conversely, the later stage is controlled by the more poorly accessible organic phase leading to low but lasting solute concentration that could explain the persistent tail in the concentrations time series of Pz28 and Pz29.

5. Conclusions

Concentrations time series of 1,1,1-TCA and 1,1-DCE in groundwater downstream of an industrial site were analyzed in this article using dissolution and transport-degradation models. Concentrations of metallic trace elements measured in groundwater are low and conditions are aerobic. Given these geochemical conditions of the water table, the 1,1-DCE is assumed to be non-reactive. In numerical models, the distribution of permeabilities and the transfer coefficient of the dual domain model are relatively simple and are certainly less accurate than the real fracture chalk geology.

Of the six tested models, the model 3 did neither fit concentration data nor the ratio of 1,1-DCE to 1,1,1-TCA. The five others fitted relatively well concentration data, and model 5 was the best model to fit well both concentration data and the ratio of 1,1-DCE to 1,1,1-TCA. This suggests thus that at this site the source is a NAPL composed by both 1,1-DCE and 1,1,1-TCA, and transport must be modelled in a heterogeneous domain. The results of the models agree with work in the literature in that the multiphasic behavior, even in the case of pollution in a single event, is dictated by the type of dissolution in a heterogeneous medium. For real sites, this type of dissolution could complicate the estimation and forecasting of remediation efforts and should therefore be taken into consideration for better characterization of pollution and the development of effective site management strategies. In particular, for remedial techniques, the reduction in mass flow for a given level of mass removal from the source is important information for evaluating the effectiveness of the treatment.

6. Author contributions

Valeureux D. Illy: Writing, Editing, Optimisation of models

Gregory Cohen: Reviewing, Editing, Validation.

Elicia Verardo: Reviewing, Technical help on the modeling software, Suggestions on the graphical presentation of the results.

Patrick Höhener: Methodology, Refinement of the objectives, Reviewing.

Nathalie Guiserix: Data curation, objectives definition.

Olivier Attéia: Model design, Modelling, Reviewing.

7. Acknowledgments

This article is published as part of a doctoral thesis funded by the RENAULT GROUP and the French ANRT.

We thank anonymous reviewers for their constructive comments.

References

Abe, Y., Aravena, R., Zopfi, J., Shouakar-Stash, O., Cox, E., Roberts, J.D., Hunkeler, D., 2009. Carbon and chlorine isotope fractionation during aerobic oxidation and reductive dechlorination of vinyl chloride and cis-1, 2-dichloroethene. *Environ. Sci. Technol.* **43**, 101–107.

Adamson, D.T., Parkin, G.F., 1999. Biotransformation of mixtures of chlorinated aliphatic hydrocarbons by an acetate-grown methanogenic enrichment culture. *Water Res.* **33**, 1482–1494.

Akyol, N.H., 2018. Surfactant-Enhanced Permanganate Oxidation on Mass-Flux Reduction and Mass Removal (MFR-MR) Relationship for Pool-Dominated TCE Source Zones in Heterogeneous Porous Media. *Water. Air. Soil Pollut.* **229**, 285. https://doi.org/10.1007/s11270-018-3946-3

Akyol, N.H., Lee, A.R., Brusseau, M.L., 2013. Impact of Enhanced-Flushing Reagents and Organic Liquid Distribution on Mass Removal and Mass Discharge Reduction. *Water. Air. Soil Pollut.* **224**, 1731. https://doi.org/10.1007/s11270-013-1731-x

Akyol, N.H., Turkkan, S., 2018. Effect of Cyclodextrin-Enhanced Dissolution on Mass Removal and Mass-Flux Reduction Relationships for Non-uniformly Organic Liquid Distribution in Heterogeneous Porous Media. *Water. Air. Soil Pollut.* **229**, 30. https://doi.org/10.1007/s11270-017-3673-1

Bae, S., Lee, W., 2010. Inhibition of nZVI reactivity by magnetite during the reductive degradation of 1, 1, 1-TCA in nZVI/magnetite suspension. *Appl. Catal. B Environ.* **96**, 10–17.

Battersby, N.S., 1990. A review of biodegradation kinetics in the aquatic environment. *Chemosphere* **21**, 1243–1284.

Bear, J., 2012. Hydraulics of groundwater. Courier Corporation.

Berner, R.A., 2015. Iron Sulfides Formed from Aqueous Solution at Low Temperatures and Atmospheric Pressure. *J. Geol.* https://doi.org/10.1086/626987

Bost, R.C., Perry, R.G., 2006. Environmental Forensic Characterization of Chlorinated Solvent DNAPL Sources.

Briggs, M.A., Day-Lewis, F.D., Ong, J.B., Harvey, J.W., Lane, J.W., 2014. Dual-domain mass-transfer parameters from electrical hysteresis: Theory and analytical approach applied to laboratory, synthetic streambed, and groundwater experiments. *Water Resour. Res.* **50**, 8281–8299.

Broholm, M.M., Hunkeler, D., Tuxen, N., Jeannottat, S., Scheutz, C., 2014. Stable carbon isotope analysis to distinguish biotic and abiotic degradation of 1, 1, 1-trichloroethane in groundwater sediments. *Chemosphere* **108**, 265–273.

Chen, N., Valdes, D., Marlin, C., Blanchoud, H., Guerin, R., Rouelle, M., Ribstein, P., 2019. Water, nitrate and atrazine transfer through the unsaturated zone of the Chalk aquifer in northern France. *Sci. Total Environ.* **652**, 927–938.

Cho, Y., Choi, S.-I., 2010. Degradation of PCE, TCE and 1, 1, 1-TCA by nanosized FePd bimetallic particles under various experimental conditions. *Chemosphere* **81**, 940–945.

Christ, J.A., Ramsburg, C.A., Pennell, K.D., Abriola, L.M., 2006. Estimating mass discharge from dense nonaqueous phase liquid source zones using upscaled mass transfer coefficients: An evaluation using multiphase numerical simulations. *Water Resour. Res.* **42**.

Clement, T.P., Kim, Y.-C., Gautam, T.R., Lee, K.-K., 2004. Experimental and numerical investigation of DNAPL dissolution processes in a laboratory aquifer model. *Groundw. Monit. Remediat.* **24**, 88–96.

Cline, P.V., Delfino, J.J., 1989. Transformation kinetics of 1, 1, 1-trichloroethane to the stable product 1, 1-dichloroethene. *Biohazards Drink. Water Treat.* 47–56.

Davis, G.B., Rayner, J.L., Trefry, M.G., Fisher, S.J., Patterson, B.M., 2005. Measurement and modeling of temporal variations in hydrocarbon vapor behavior in a layered soil profile. *Vadose Zone J.* **4**, 225–239.

De Best, J.H., Hage, A., Doddema, H.J., Janssen, D.B., Harder, W., 1999. Complete transformation of 1, 1, 1-trichloroethane to chloroethane by a methanogenic mixed population. *Appl. Microbiol. Biotechnol.* **51**, 277–283.

DiFilippo, E.L., Carroll, K.C., Brusseau, M.L., 2010. Impact of organic-liquid distribution and flow-field heterogeneity on reductions in mass flux. *J. Contam. Hydrol.* **115**, 14–25.

Duhamel, M., Wehr, S.D., Yu, L., Rizvi, H., Seepersad, D., Dworatzek, S., Cox, E.E., Edwards, E.A., 2002. Comparison of anaerobic dechlorinating enrichment cultures maintained on tetrachloroethene, trichloroethene, cis-dichloroethene and vinyl chloride. *Water Res.* **36**, 4193–4202.

Ellenrieder, W., Reinhard, M., 1988. ATHIAS—an information system for abiotic transformations of halogenated hydrocarbons in aqueous solution. *Chemosphere* **17**, 331–344.

Elsner, M., Chartrand, M., VanStone, N., Lacrampe Couloume, G., Sherwood Lollar, B., 2008. Identifying abiotic chlorinated ethene degradation: characteristic isotope patterns in reaction products with nanoscale zero-valent iron. *Environ. Sci. Technol.* **42**, 5963–5970.

Falta, R.W., 2003. Modeling sub-grid-block-scale dense nonaqueous phase liquid (DNAPL) pool dissolution using a dual-domain approach. *Water Resour. Res.* **39**.

Falta, R.W., Basu, N., Rao, P.S., 2005b. Assessing impacts of partial mass depletion in DNAPL source zones: II. Coupling source strength functions to plume evolution. *J. Contam. Hydrol.* **79**, 45–66.

Falta, R.W., Rao, P.S., Basu, N., 2005a. Assessing the impacts of partial mass depletion in DNAPL source zones: I. Analytical modeling of source strength functions and plume response. *J. Contam. Hydrol.* **78**, 259–280.

Fennelly, J.P., Roberts, A.L., 1998. Reaction of 1, 1, 1-trichloroethane with zero-valent metals and bimetallic reductants. *Environ. Sci. Technol.* **32**, 1980–1988.

Ferrey, M.L., Wilkin, R.T., Ford, R.G., Wilson, J.T., 2004. Nonbiological removal of cis-dichloroethylene and 1, 1-dichloroethylene in aquifer sediment containing magnetite. *Environ. Sci. Technol.* **38**, 1746–1752.

Fure, A.D., Jawitz, J.W., Annable, M.D., 2006. DNAPL source depletion: Linking architecture and flux response. *J. Contam. Hydrol.* **85**, 118–140.

Gander, J.W., Parkin, G.F., Scherer, M.M., 2002. Kinetics of 1, 1, 1-trichloroethane transformation by iron sulfide and a methanogenic consortium. *Environ. Sci. Technol.* **36**, 4540–4546.

Gauthier, T.D., Murphy, B.L., 2003. Age dating groundwater plumes based on the ratio of 1, 1-dichloroethylene to 1, 1, 1-trichloroethane: An uncertainty analysis. *Environ. Forensics* **4**, 205–213.

Génin, J.-M.R., Bourrié, G., Trolard, F., Abdelmoula, M., Jaffrezic, A., Refait, P., Maitre, V., Humbert, B., Herbillon, A., 1998. Thermodynamic Equilibria in Aqueous Suspensions of Synthetic and Natural Fe(II)−Fe(III) Green Rusts: Occurrences of the Mineral in Hydromorphic Soils. *Environ. Sci. Technol.* **32**, 1058–1068. https://doi.org/10.1021/es970547m

Gerkens, R.R., Franklin, J.A., 1989. The rate of degradation of 1, 1, 1-trichloroethane in water by hydrolysis and dehydrochlorination. *Chemosphere* **19**, 1929–1937.

Greskowiak, J., Prommer, H., Liu, C., Post, V.E.A., Ma, R., Zheng, C., Zachara, J.M., 2010. Comparison of parameter sensitivities between a laboratory and field-scale model of uranium transport in a dual domain, distributed rate reactive system. *Water Resour. Res.* **46**.

Grostern, A., Edwards, E.A., 2009. Characterization of a Dehalobacter coculture that dechlorinates 1, 2-dichloroethane to ethene and identification of the putative reductive dehalogenase gene. *Appl. Environ. Microbiol.* **75**, 2684–2693.

Grostern, A., Edwards, E.A., 2006. A 1, 1, 1-trichloroethane-degrading anaerobic mixed microbial culture enhances biotransformation of mixtures of chlorinated ethenes and ethanes. *Appl. Environ. Microbiol.* **72**, 7849–7856.

Haag, W.R., Mill, T., 1988. Effect of a subsurface sediment on hydrolysis of haloalkanes and epoxides. *Environ. Sci. Technol.* **22**, 658–663.

Hashimoto, A., Iwasaki, K., Nakasugi, N., Nakajima, M., Yagi, O., 2002. Degradation pathways of trichloroethylene and 1, 1, 1-trichloroethane by Mycobacterium sp. TA27. *Biosci. Biotechnol. Biochem.* **66**, 385–390.

Hunkeler, D., Meckenstock, R.U., Lollar, B.S., Schmidt, T.C., Wilson, J.T., 2008. A guide for assessing biodegradation and source identification of organic ground water contaminants using compound specific isotope analysis (CSIA). EPA/600/R-08/148. *USEPA Publ* 1–82.

Karadimitriou, N.K., Joekar-Niasar, V., Babaei, M., Shore, C.A., 2016. Critical role of the immobile zone in non-Fickian two-phase transport: A new paradigm. *Environ. Sci. Technol.* **50**, 4384–4392.

Kota, S., Trione, C.W., Goldstein, K.J., Wang, J.Y., 2003. Re-evaluation of treatment approach for a site contaminated with Freon-113 and 1, 1, 1-trichloroethane. *Remediat. J. J. Environ. Cleanup Costs Technol. Tech.* **13**, 17–27.

Lari, K.S., Davis, G.B., Rayner, J.L., Bastow, T.P., Puzon, G.J., 2019. Natural source zone depletion of LNAPL: A critical review supporting modelling approaches. *Water Res.* **157**, 630–646.

Lawrence, S.J., 2006. Description, Properties, and Degradation of Selected Volatile Organic Compounds Detected in Ground Water–A Review of Selected Literature.

Lemke, L.D., Abriola, L.M., 2006. Modeling dense nonaqueous phase liquid mass removal in nonuniform formations: Linking source-zone architecture and system response. *Geosphere* **2**, 74–82.

Lexman, A., 2016. Carte des départements - data.gouv.fr [WWW Document]. URL https://www.data.gouv.fr/fr/datasets/carte-des-departements-2-1/ (accessed 8.31.21).

Löffler, F.E., Edwards, E.A., 2006. Harnessing microbial activities for environmental cleanup. *Curr. Opin. Biotechnol.* **17**, 274–284.

Major, D.W., McMaster, M.L., Cox, E.E., Edwards, E.A., Dworatzek, S.M., Hendrickson, E.R., Starr, M.G., Payne, J.A., Buonamici, L.W., 2002. Field demonstration of successful bioaugmentation to achieve dechlorination of tetrachloroethene to ethene. *Environ. Sci. Technol.* **36**, 5106–5116.

McCarty, P.L., 1997. Breathing with chlorinated solvents. *Science* **276**, 1521–1522.

Morrison, R.D., Murphy, B.L., 2002. Chlorinated solvents: Chemistry, history, and utilization for source identification and age dating. *Introd. Environ. Forensics* 261–310.

Nambi, I.M., Powers, S.E., 2000. NAPL dissolution in heterogeneous systems: an experimental investigation in a simple heterogeneous system. *J. Contam. Hydrol.* **44**, 161–184.

Neumann, R.B., LaBolle, E.M., Harvey, C.F., 2008. The Effects of Dual-Domain Mass Transfer on the Tritium- Helium-3 Dating Method. *Environ. Sci. Technol.* **42**, 4837–4843.

Palau, J., Jamin, P., Badin, A., Vanhecke, N., Haerens, B., Brouyère, S., Hunkeler, D., 2016. Use of dual carbon–chlorine isotope analysis to assess the degradation pathways of 1, 1, 1-trichloroethane in groundwater. *Water Res.* **92**, 235–243.

Palau, J., Shouakar-Stash, O., Hunkeler, D., 2014. Carbon and chlorine isotope analysis to identify abiotic degradation pathways of 1, 1, 1-trichloroethane. *Environ. Sci. Technol.* **48**, 14400–14408.

Plumb Jr, R.H., 1992. The importance of volatile organic compounds as a disposal site monitoring parameter. In 'Groundwater Contamination and Analysis at Hazardous Waste Sites'. Marcel Dekker New York, pp. 173–197.

Powers, S.E., Abriola, L.M., Dunkin, J.S., Weber Jr, W.J., 1994. Phenomenological models for transient NAPL-water mass-transfer processes. *J. Contam. Hydrol.* **16**, 1–33.

Powers, S.E., Abriola, L.M., Weber Jr, W.J., 1992. An experimental investigation of nonaqueous phase liquid dissolution in saturated subsurface systems: Steady state mass transfer rates. *Water Resour. Res.* **28**, 2691–2705.

Ramsburg, C.A., Thornton, C.E., Christ, J.A., 2010. Degradation product partitioning in source zones containing chlorinated ethene dense non-aqueous-phase liquid. *Environ. Sci. Technol.* **44**, 9105–9111.

Rivett, M.O., Allen-King, R.M., 2003. A controlled field experiment on groundwater contamination by a multicomponent DNAPL: dissolved-plume retardation. *J. Contam. Hydrol.* **66**, 117–146.

Rivett, M.O., Feenstra, S., Cherry, J.A., 2001. A controlled field experiment on groundwater contamination by a multicomponent DNAPL: creation of the emplaced-source and overview of dissolved plume development. *J. Contam. Hydrol.* **49**, 111–149.

Scheutz, C., Durant, N. d, Dennis, P., Hansen, M.H., Jørgensen, T., Jakobsen, R., Cox, E.E., Bjerg, P.L., 2008. Concurrent ethene generation and growth of Dehalococcoides containing vinyl chloride reductive dehalogenase genes during an enhanced reductive dechlorination field demonstration. *Environ. Sci. Technol.* **42**, 9302–9309.

Scheutz, C., Durant, N.D., Hansen, M.H., Bjerg, P.L., 2011a. Natural and enhanced anaerobic degradation of 1, 1, 1-trichloroethane and its degradation products in the subsurface–a critical review. *Water Res.* **45**, 2701–2723.

Scheutz, C., Durant, N.D., Hansen, M.H., Bjerg, P.L., 2011b. Natural and enhanced anaerobic degradation of 1, 1, 1-trichloroethane and its degradation products in the subsurface–a critical review. *Water Res.* **45**, 2701–2723.

Snyder, J.T., 1990. Aqueous Degreasing A Viable Alternative to Vapor Degreasing. In 'Solvent Substitution: A Proceedings/Compendium of Papers: Based on the First Annual International Workshop on Solvent Substitution, December 4-7, 1990, Phoenix, Arizona'. US Department of Energy, Office of Technology Development, Environmental …, p. 174.

Sun, B., Griffin, B.M., Ayala-del-Río, H.L., Hashsham, S.A., Tiedje, J.M., 2002. Microbial dehalorespiration with 1, 1, 1-trichloroethane. *Science* **298**, 1023–1025.

VanStone, N., Elsner, M., Lacrampe-Couloume, G., Mabury, S., Sherwood Lollar, B., 2008. Potential for identifying abiotic chloroalkane degradation mechanisms using carbon isotopic fractionation. *Environ. Sci. Technol.* **42**, 126–132.

Vogel, T.M., McCARTY, P.L., 1987. Rate of abiotic formation of 1, 1-dichloroethylene from 1, 1, 1-trichloroethane in groundwater. *J. Contam. Hydrol.* **1**, 299–308.

Wefer-Roehl, A., Graber, E.R., Borisover, M.D., Adar, E., Nativ, R., Ronen, Z., 2001. Sorption of organic contaminants in a fractured chalk formation. *Chemosphere* **44**, 1121–1130.

675 Wing, M.R., 1997. Apparent first-order kinetics in the transformation of 1, 1, 1-trichloroethane
676 in groundwater following a transient release. *Chemosphere* **34**, 771–781.
677 Wu, X., Lu, S., Qiu, Z., Sui, Q., Lin, K., Du, X., Luo, Q., 2014. The reductive degradation of
678 1,1,1-trichloroethane by Fe(0) in a soil slurry system. *Environ. Sci. Pollut. Res.* **21**,
679 1401–1410. https://doi.org/10.1007/s11356-013-2029-7
680 Yang, Q., Li, Y., Zhou, J., Xie, X., Su, Y., Gu, Q., Kamon, M., 2013. Modelling of benzene
681 distribution in the subsurface of an abandoned gas plant site after a long term of
682 groundwater table fluctuation. *Hydrol. Process.* **27**, 3217–3226.
683 Zheng, C., Wang, P.P., 1999. MT3DMS: a modular three-dimensional multispecies transport
684 model for simulation of advection, dispersion, and chemical reactions of contaminants
685 in groundwater systems; documentation and user's guide.
686 Zhu, J., Sykes, J.F., 2004. Simple screening models of NAPL dissolution in the subsurface.
687 *J. Contam. Hydrol.* **72**, 245–258.
688
689
690
691
692
693
694
695
696
697
698
699
700
701
702
703
704
705
706
707
708
709
710
711
712
713
714
715
716
717
718
719
720
721
722
723
724
725
726